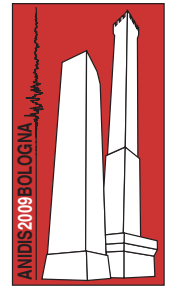


# Some proposals for the evaluation of non-linear structural response based on seismic hazard disaggregation

L. Elefante, F. Jalayer, I. Iervolino, G. Manfredi

*Dipartimento di Ingegneria Strutturale, Università di Napoli Federico II, Napoli, Italia*



*Keywords: Seismic Assessment, Ground Motion, Weighted Regression, Seismic Hazard Disaggregation.*

## ABSTRACT

Alternative non-linear dynamic analysis procedures, using real ground motion records, can be employed to carry out probability-based seismic assessments. The results of seismic hazard disaggregation can be used to assign relative plausibility values (weights) to a given ground motion record based on its corresponding magnitude, distance, and deviation from the attenuation prediction (epsilon). These relative plausibility values can be used to weight the ground motion records used for non-linear dynamic analyses for different levels of intensity measure. The weighted records can be implemented in non-linear dynamic analysis procedure both for a wide range of ground motion intensities and also for a limited range of ground motion intensities. The implication of using the weighted ground motion records is studied in terms of the annual frequency of exceedance of the critical component demand to capacity in an existing reinforced concrete structure using both the first-mode spectral acceleration and the peak ground acceleration as intensity measures. It is demonstrated that the resulting annual frequencies based on weighted records are comparable to those obtained by using vector intensity measures.

## 1 INTRODUCTION

The seismic input selection represents one of the main issues in assessing the seismic response of a structure through numerical dynamic analysis. It is reasonable to choose ground motion records whose magnitude, distance, site conditions and mechanisms of fault are representative for the site of structure under consideration. This choice may be guided by the disaggregation of the seismic hazard (Bazzurro and Cornell, 1999) for the site of interest. However, once chosen the set of records, there are several techniques to evaluate the structural seismic response.

In this paper we show how the results of the hazard disaggregation can be used to assign weights to selected records according to the characteristics such as magnitude, distance and deviation from the attenuation prediction (epsilon -  $\epsilon$ ). Weighting the effects of each ground motion, in terms of annual frequency of exceedance of a parameter of demand expressed in terms of the

critical component demand to capacity, permits more accurate estimation of the structural response with a limited number of analysis.

## 2 PROBABILISTIC ASSESSMENTS BASED ON NON-LINEAR DYNAMIC ANALYSIS

A probabilistic performance-based criterion for seismic assessment of existing structures can be written as:

$$\lambda_{DM} \leq P_0 \quad (1)$$

where  $\lambda_{DM}$  refers to the (mean) annual frequency of exceeding a specified damage level related to the *damage measure* (DM) and  $P_0$  is the allowable probability threshold for the assessment. In order to calculate  $\lambda_{DM}$  using non-linear time-history analyses, it is common to use an intermediate parameter known as the ground motion *intensity measure* (IM) in order to relate the characteristics of ground motion record to the structural performance.

The annual rate of exceeding a specified limit state can be expanded, using the principles of

probability theory, with respect to the adopted (scalar) IM in the following:

$$\lambda_{DM}(y) = \int P_{DM|IM}(DM > y|x) d\lambda_{IM}(x) \quad (2)$$

The first term in the integrand  $P_{DM|IM}(DM > y|x)$  is the conditional probability of exceeding the damage threshold  $y$  for a given value of  $IM = x$ . This term is also known as the structural *fragility*. The second term in the integrand is the absolute value of the derivative of the annual rate of exceeding  $IM = x$ ; this second term is known as the *hazard* for the adopted IM. Ideally, the hazard function for the adopted IM is obtained from the results of site-specific probabilistic seismic hazard analysis (PSHA, see McGuire 2004). In lieu of site-specific PSHA results, the national seismic maps can be used to obtain the annual rates of exceedance for various IM levels.

The non-linear dynamic analysis procedures based on a limited suite of ground motion records can be used to estimate the fragility term in the integrand in equation (2). Depending on the amount of structural analysis and also the range of limit states for which the performance assessment is done, two alternative non-linear dynamic analysis procedures are considered in this work, the *cloud* methods and the *stripes* methods (Jalayer and Cornell 2008, Baker 2007). The cloud method employs the linear least squares scheme to the specified DM based on non-linear structural response for a suite of ground motion records (un-scaled) in order to estimate the conditional mean and standard deviation of DM given IM. Moreover, by assuming that the errors from the least square estimate are independent and identically distributed (i.i.d.), the  $P_{DM|IM}(DM > y|x)$  can be estimated. Alternatively, the stripes method employs the non-linear structural response parameters for the suite of records that are scaled to successively increasing IM levels, this is referred to as *the stripe response*. Subsequently, the statistical properties of the stripe responses for various IM levels, calculated based on the response to the suite of records, can be employed to obtain the probability of exceeding a specified damage level.

In the case where a vector-valued  $IM = [IM_1, IM_2]$  consisting of two scalar IM's is adopted, the fragility term in equation (2) for the annual rate of exceeding  $DM = y$  can be expanded with respect to  $IM_2$  and re-arranged as following:

$$\lambda_{DM}(y) = \iint P_{DM|IM_1, IM_2}(DM > y|x, z) \cdot P_{IM_2|IM_1}(z|x) d\lambda_{IM_1}(x) \quad (3)$$

The first term in the integrand is the conditional probability of exceeding  $DM = y$  given  $IM_1$  and  $IM_2$  and the second term is the conditional probability density function (PDF) for  $IM_2 = z$  given  $IM_1 = x$ . Similar to the case regarding scalar IM, both cloud method and stripes method can be employed in order to perform probabilistic assessments. In the context of cloud method, the two-variable linear least squares scheme can be used to estimate the statistical parameters for the damage measure conditioned on both  $IM_1$  and  $IM_2$ . Alternatively, using the stripes methods, the simple linear least squares can be applied to the stripe response at various  $IM_1$  level with  $IM_2$  as the independent variable.

### 2.1 Accounting for collapse in multiple-stripe analysis

As described above using the stripes methods, records are scaled to the primary IM parameter and then regression analysis is used on the stripe of data to determine the effect of the secondary IM parameter. Logistic regression is used to compute the probability of collapse, and linear regression is used to model the non-collapsing responses. Rather than estimating the probability of collapse simply as the fraction of records at an  $IM_1$  stripe that cause collapse, probability of collapse is calculated using logistic regression (Neter et al. 1996). Using the indicator variable  $C$  to designate occurrence of collapse ( $C$  equals 1 if the record causes collapse and 0 otherwise), the following functional form is fitted:

$$P(C|IM_1 = x, IM_2 = z) = \frac{e^{a(x)+b(x) \cdot z}}{1 + e^{a(x)+b(x) \cdot z}} \quad (4)$$

where  $a$  and  $b$  are coefficients to be estimated from regression on the record set that has been scaled to  $IM_1 = x$ . Using the total probability theorem the first term in the integrand of equation (3) can be expanded in this way:

$$P_{DM|IM_1, IM_2}(DM > y|x, z) = P_{DM|IM_1, IM_2}(DM > y|x, z, NC) \cdot P(NC|IM_1 = x, IM_2 = z) + 1 \cdot P(C|IM_1 = x, IM_2 = z) \quad (5)$$

where:

$$P(NC|IM_1 = x, IM_2 = z) = 1 - P(C|IM_1 = x, IM_2 = z) \quad (6)$$

### 3 STRUCTURAL MODEL

As the case-study, an existing school structure in the city of Avellino, Italy is considered herein. Avellino is located in the Irpinia region, where the 1980 Irpinia Earthquake with Mw 6.9 has taken place. The structure consists of three stories and a semi-embedded story and its foundation lies on stiff soil (category B according to the Italian code). For the structure in question, the original design notes and graphics have been gathered. The building is constructed in the 1960's and it is designed for gravity loads only, as it is frequently encountered in the post second world war construction. In Figure 1a, the tri-dimensional view of the structure is illustrated; it can be observed that the building is highly irregular both in plane and elevation.

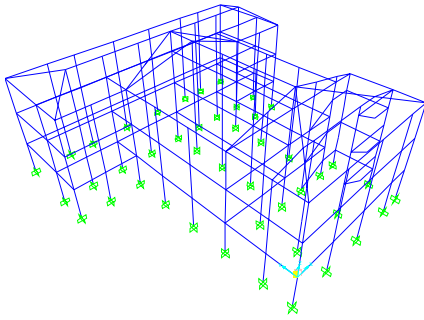


Figure 1. The tri-dimensional view of the scholastic building.

The main central frame in the structure is extracted and used as the structural model (Figure 2).

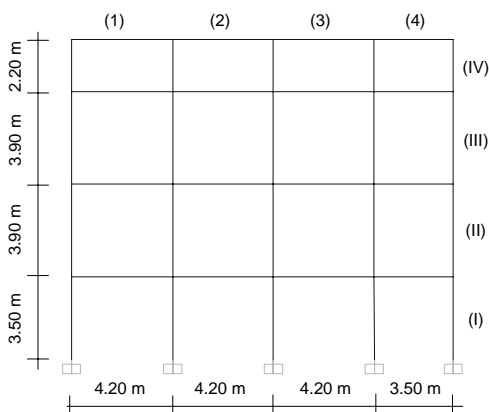


Figure 2. The central of the case-study building.

The columns have rectangular section with the following dimensions: first storey:  $40 \times 55 \text{ cm}^2$ , second storey:  $40 \times 45 \text{ cm}^2$ , third storey:  $40 \times 40 \text{ cm}^2$ , and fourth storey:  $30 \times 40 \text{ cm}^2$ . The beams, also with rectangular section, have the following dimensions:  $40 \times 70 \text{ cm}^2$  at first and second floor,

and  $30 \times 50 \text{ cm}^2$  for the ultimate two floors. It can be inferred from the original design notes that the steel rebar is of the type Aq40 and the concrete has a minimum resistance equal to  $180 \text{ kg/cm}^2$  (R.D.L. 2229, 1939). The finite element model of the frame is constructed assuming that the non-linear behavior in the structure is concentrated in plastic hinges located at the element ends (lumped plasticity). The plastic hinges are defined by moment-curvature relation which is derived by analyzing the reinforced concrete section at the hinge location. In this study, the section analysis is based on the Mander-Priestly (Mander et al., 1988) constitutive relation for reinforced concrete assuming that the concrete is not confined and the reinforcing steel behavior is elastic-plastic. The behavior of the plastic hinge is characterized by four phases, namely: rigid phase, cracked phase, post-yielding phase and post-peak phase. In addition to flexural deformation, the yielding rotation take into account also the shear deformation and the deformation related to bar slip based on the code recommendations. As it regards the post-peak behavior, it is assumed that the section resistance drops to zero, resulting in a tri-linear curve (Figure 3).

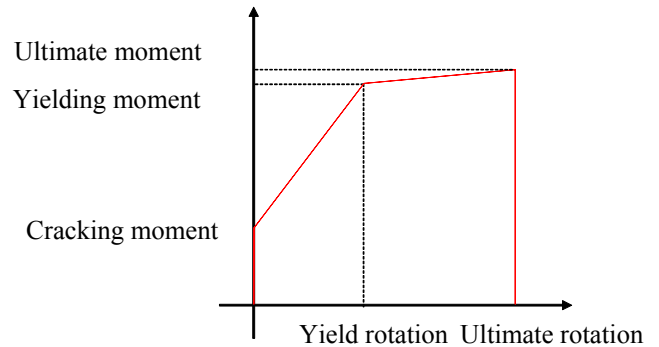


Figure 3. Schematic diagram of the typical tri-linear behavior characterizing the rigid-plastic hinge.

The finite element model of the structure is constructed using the OPENSEES software employing the force-based *beam with hinges* model (Scott and Fenves, 2006). This type of element consists of three parts. Two hinges at the ends, and a linear-elastic region in the middle. The length of the two hinges at the ends is approximated by the semi-empirical formulas provided for the plastic hinge length in the Italian code (OPCM 3431, 2005, now superseded) which take into account both the effect of shear and bar slip in the (post-peak) ultimate phase of the section behavior. The plastic hinges take into account the superposition of both flexural and axial action. The structural damping is modeled based on the Rayleigh model and is assumed to

be equal to 5% for the first two modes. The small amplitude period for the first two vibration modes are equal to 0.73 and 0.26 seconds respectively.

#### 4 THE SUITES OF GROUND MOTION RECORDS AND THEIR PROPERTIES

Two different suites, respectively of 21 (*Sel\_A*) and 20 (*Sel\_B*) ground motion records, have been selected for this study. They are all main-shock recordings and include only one of the horizontal components of the same registration. The soil category on which the ground motions are recorded is stiff soil ( $400 \text{ m/s} < V_{s30} < 700 \text{ m/s}$ ) which is consistent with the soil-type for the site. The epsilon values are calculated using the ground motion prediction relation of Sabetta and Pugliese (Sabetta and Pugliese, 1996).

##### 4.1 Record selection A (*Sel\_A*)

The first suite is based on Mediterranean events taken from European Ground motion database (17 recordings) and NGA (4 recordings). The earthquake events have moment magnitude between 5.3 and 7.2, covering quite completely the interval. The records have closest distances ranging between 7km and 30km. Table 1 illustrates the ground motion recordings, their moment magnitude ( $M_w$ ), epicentral distance (ED), PGA,  $S_a(T_1)$  and epsilon  $\epsilon$  values for each record.

Table 1. Selection A of ground motion records.

| Record            | $M_w$ | ED<br>[km] | $S_a(T_1)$<br>[g] | PGA<br>[g] | $\epsilon$ |
|-------------------|-------|------------|-------------------|------------|------------|
| Basso Tirreno     | 6.0   | 18         | 0.17              | 0.15       | -0.121     |
| Valnerina         | 5.8   | 23         | 0.03              | 0.04       | -0.529     |
| Camp. Lucano      | 6.9   | 16         | 0.31              | 0.16       | -0.519     |
| Preveza           | 5.4   | 28         | 0.10              | 0.14       | -0.244     |
| Umbria Marche     | 5.6   | 19         | 0.02              | 0.21       | 0.230      |
| Lazio Abruzzo     | 5.9   | 36         | 0.05              | 0.07       | -0.219     |
| Etolia            | 5.3   | 20         | 0.01              | 0.04       | -0.518     |
| Montenegro        | 5.4   | 18         | 0.09              | 0.07       | -0.227     |
| Kyllini           | 5.9   | 14         | 0.15              | 0.15       | -0.231     |
| Duzce 1           | 7.2   | 26         | 0.18              | 0.13       | -0.722     |
| Umbria Marche     | 5.7   | 32         | 0.05              | 0.04       | -0.334     |
| Potenza           | 5.8   | 28         | 0.08              | 0.10       | -0.003     |
| Ano Liosia        | 6.0   | 20         | 0.06              | 0.16       | -0.308     |
| Adana             | 6.3   | 39         | 0.05              | 0.03       | -0.749     |
| South Iceland     | 6.5   | 15         | 0.13              | 0.21       | -0.344     |
| Tithorea          | 5.9   | 25         | 0.02              | 0.03       | -0.639     |
| Patras            | 5.6   | 30         | 0.02              | 0.05       | -0.184     |
| Friuli Italy-01   | 6.5   | 20         | 0.35              | 0.35       | 0.168      |
| Friuli, Italy-02  | 5.9   | 18         | 0.08              | 0.21       | 0.110      |
| Friuli, Italy-03  | 5.5   | 20         | 0.21              | 0.11       | 0.034      |
| Irpinia, Italy-01 | 6.9   | 15         | 0.30              | 0.13       | -0.466     |
| (average)         | 6.0   | 23         | 0.12              | 0.12       | -0.277     |

The acceleration spectra for the original (un-scaled) records are plotted in Figure 4.

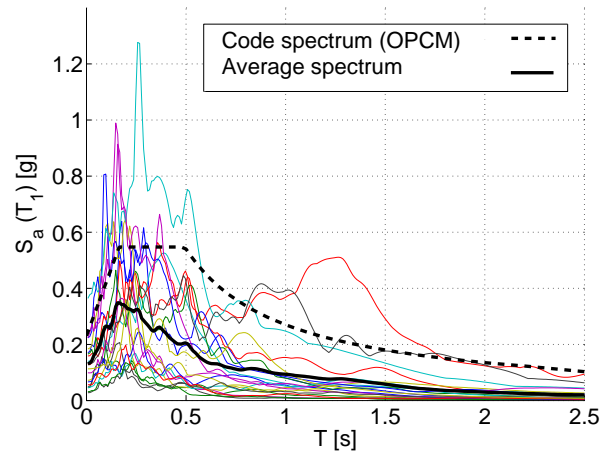


Figure 4. Acceleration Spectra *Sel\_A*.

##### 4.2 Record selection B (*Sel\_B*)

The second suite is based on Mediterranean events all taken from European Ground motion database. The earthquake events have moment magnitude between 5.9 and 7.2. The records have closest distances ranging between 0km and 71km. Table 2 illustrates the ground motion recordings, their moment magnitude ( $M_w$ ), epicentral distance (ED), PGA,  $S_a(T_1)$  and epsilon  $\epsilon$  values for each record.

Table 2. Selection B of ground motion records.

| Record        | $M_w$ | ED<br>[km] | $S_a(T_1)$<br>[g] | PGA<br>[g] | $\epsilon$ |
|---------------|-------|------------|-------------------|------------|------------|
| Friuli        | 6.5   | 42         | 0.22              | 0.06       | -0.015     |
| Friuli        | 6.5   | 87         | 0.11              | 0.05       | 0.003      |
| Camp. Lucano  | 6.9   | 48         | 0.25              | 0.11       | -0.204     |
| Camp. Lucano  | 6.9   | 16         | 0.31              | 0.16       | -0.493     |
| Kalamata      | 5.9   | 10         | 0.48              | 0.22       | -0.231     |
| Kalamata      | 5.9   | 11         | 0.48              | 0.24       | -0.233     |
| Umbria Marche | 6.0   | 11         | 0.56              | 0.52       | -0.216     |
| Umbria Marche | 6.0   | 38         | 0.17              | 0.09       | 0.062      |
| South Iceland | 6.5   | 7          | 0.54              | 0.63       | -0.288     |
| Duzce 1       | 7.2   | 26         | 0.18              | 0.13       | -0.893     |
| Friuli        | 6.5   | 42         | 0.25              | 0.09       | 0.031      |
| Friuli        | 6.5   | 87         | 0.12              | 0.07       | -0.002     |
| Camp. Lucano  | 6.9   | 48         | 0.26              | 0.14       | -0.187     |
| Camp. Lucano  | 6.9   | 16         | 0.31              | 0.18       | -0.484     |
| Kalamata      | 5.9   | 10         | 0.63              | 0.30       | -0.120     |
| Kalamata      | 5.9   | 11         | 0.51              | 0.27       | -0.208     |
| Umbria Marche | 6.0   | 11         | 0.64              | 0.46       | -0.156     |
| Umbria Marche | 6.0   | 38         | 0.18              | 0.10       | 0.065      |
| South Iceland | 6.5   | 7          | 0.74              | 0.51       | -0.154     |
| Duzce 1       | 7.2   | 26         | 0.14              | 0.16       | -1.004     |
| (average)     | 6.4   | 30         | 0.35              | 0.22       | -0.236     |

The acceleration spectra for the original (un-scaled) records are plotted in Figure 5.

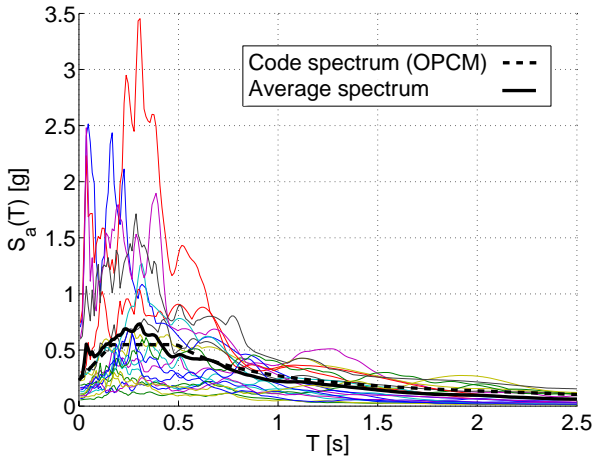


Figure 5. Acceleration Spectra *Sel\_B*.

It has to be noted that epsilon values of record selection B are all included in an interval between -1.1 and 0.07, covering quite completely the interval.

## 5 THE INTENSITY MEASURES FOR PREDICTING STRUCTURAL RESPONSE

The intensity measures (IM) can be considered as parameters or a vector of parameters that help quantifying the structural response to a ground motion. In this work, both scalar and vector IM's are studied. As scalar IM's, the peak ground acceleration (PGA) and the spectral acceleration at the first mode denoted as  $S_a(T_1)$  are considered. As vector IM's, the pairs consisting of PGA and magnitude, [PGA,M], and  $S_a(T_1)$  and epsilon  $\varepsilon$  of the attenuation law, [ $S_a(T_1), \varepsilon$ ], are considered. PGA has been most commonly used as the ground motion intensity measure in the past. On the other hand, recently,  $S_a(T_1)$  is considered and verified to be a more suitable choice of an IM, as it reflects the elastic response of an SDOF system with a period equal to the small-amplitude first-mode period of the structure. However, it is unable to reflect the effect of larger frequencies (higher modes in a structure with several degrees of freedom) or smaller frequencies (severe non-linear behavior in the structural elements) or the near-source effects (a single low frequency pulse dominates the ground motion record). Ideally, one should use a vector consisting of  $S_a(T_1)$  and the spectral shape  $R(T) = S_a(T)/S_a(T_1)$  where  $T$  is the second period whose spectral value is considered as important to the structural response. It has been demonstrated that the parameter epsilon of the

attenuation relation is able to act as a proxy for the spectral shape (Baker and Cornell, 2005).

## 6 THE STRUCTURAL ENGINEERING PARAMETERS

It is desirable to express the performance objective in terms of a (scalar) system damage measure which reflects how far away the structure is from the threshold of the limit state (Jalayer et al. 2007), namely:

$$\lambda_{LS} = \lambda_{DV>1} \leq P_0 \quad (7)$$

The decision variable can be defined as the ratio of system demand  $D$  to system capacity  $C_{LS}$ , (e.g., ratio of  $\theta_{max}$  to  $\theta_{CLS}$ ) or it can be defined as a functional of component demand and capacities, which is equal to one at the onset of failure. This latter formulation is the one adopted in this work. In this work the scalar system decision variable, denoted by  $Y$ , is defined as the demand to capacity ratio of the critical component, i.e., that component that brings the system closer to failure:

$$Y = \max_{l=1}^{N_{mech}} \min_{j=1}^{N_l} \frac{D_{jl}}{C_{jl}} \quad (8)$$

where  $N_{mech}$  is the number of considered potential failure mechanisms and  $N_l$  is the number of components taking part in the  $l^{th}$  mechanism. This corresponds to the system reliability concept of *cut-set* (Ditlevsen and Madsen, 1996), defined as any set of components whose joint failure,  $Y_l = \min_{j=1}^{N_l} D_{jl}/C_{jl}$ , implies the failure of the system,  $Y = \max_{l=1}^{N_{mech}} Y_l$ .

## 7 GROUND MOTION RECORD SELECTION AND SUFFICIENCY

A preferred IM is both "sufficient" with respect to the ground motion characteristics and also "efficient". A sufficient intensity measure renders the structural response conditionally statistically independent of other ground motion characteristics (Iervolino and Cornell, 2005), while an efficient intensity measure predicts the structural response with (relatively) small record-to-record variability.

The efficiency of the candidate IM can be measured by the variability in the residuals of the regression analysis. In order to establish sufficiency, the effectiveness of ground motion characteristic variables as additional regression

variables, can be investigated. In other words, ground motion characteristic variables cause very little improvement in the regression prediction as regression variables in addition to a “sufficient” intensity measure. This improvement may be judged by the reduction in the dispersion of the regression residuals and/or the statistical significance of the regression coefficients corresponding to the ground motion characteristic variables.

## 8 THE WEIGHTED CLOUD METHOD

Using a weighted regression scheme (Weisberg, 1985) may help in reducing the dependence of the residuals (of the “original” regression on  $IM_1$ ) on  $IM_2$ . It should be recalled that regression analysis works by minimizing the sum of the squared errors (residuals) between the observed DM and the predicted DM. The weighted regression scheme weights each error term (residual) proportional to its corresponding variance. A similar weighting scheme is implemented in this work in order to adjust the residuals (of the “original” regression of DM on  $IM_1$ ) with regard to their dependence on  $IM_2$ .

It can be argued that the variance of each error term and hence the corresponding weight is positively related to the following ratio:

$$w_i \propto \frac{P_{IM_2|IM_1}(z_i|x)_{disaggregation}}{P_{IM_2|IM_1}(z_i|x)_{data}} \quad (9)$$

where  $P_{IM_2|IM_1}(z|x)$  is the fraction of the ground motions with  $IM_2$  equal to  $z$  for a given  $IM_1$  equal to  $x$ . For the suite of record used in this work,  $P_{IM_2|IM_1}(z_i|x)_{data}$  is equal to  $1/N_T$ , where  $N_T$  is the total number of records.  $P_{IM_2|IM_1}(z_i|x)_{disaggregation}$  is the fraction of records with  $IM_2$  equal to  $z_i$  for a given  $IM_1$  equal to  $x$ , estimated from the disaggregation of hazard.

## 9 BINS IN MULTIPLE-STRIPE ANALYSIS

A similar procedure to the one used in the weighted cloud method can be implemented in the framework of multiple-stripe analysis. In fact, selected a set of records with a range of  $IM_2$  values one could re-weight the data after scaling to  $IM_1$  in relation to the disaggregation of hazard of  $IM_2|IM_1$  at each  $IM_1$  level. This method has been proposed by Shome and Cornell (1999,) and

Jalayer (2003). After discretizing  $IM_2$  into a set of “bins,” the weight for a record with an  $IM_2$  value in bin  $j$  would be:

$$w_j \propto \frac{P_{IM_2|IM_1}(z_j|x)}{n_j} \quad (10)$$

where  $P_{IM_2|IM_1}(z_j|x)$  is the probability that  $IM_2$  is equal to  $z$  (in bin  $j$ ) given  $IM_1$  equal to  $x$ , obtained from disaggregation, and  $n_j$  is the number of records in the set with  $IM_2$  in bin  $j$ . Note that for using this method it is necessary to have records in every  $IM_2$  bin considered.

## 10 NUMERICAL RESULTS

Distinguished by number of analysis carried out, two alternative procedures are considered in this work: the cloud method and the multiple-stripe method.

### 10.1 Cloud Method

#### 10.1.1 Record selection A (*Sel\_A*)

For record selection A (*Sel\_A*) the primary intensity measure used in this study in a scalar form is the peak ground acceleration (PGA), paired in vector form, with magnitude (M).

In Figure 6 the results obtained using the cloud method for the PGA and D/C data pairs are shown.

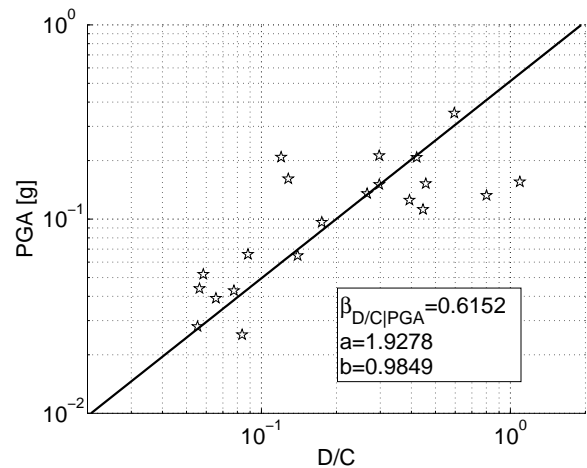


Figure 6. Simple regression PGA-D/C (*Sel\_A*).

As mentioned previously, in order to establish sufficiency of the primary intensity measure and the effectiveness of ground motion characteristic variables as additional regression variables, a graphical statistical tool known as the residual-residual plot is used. Through hypotheses test it is possible to assess whether the regression of the residuals has a statistically significant trend or

not, and if the intensity measure introduced reduces the variability of results than the original prediction of regression. In Figure 7 the residual-residual plot related to the introduction of magnitude as additional intensity measure, and the p-values calculated for the hypotheses test are shown.

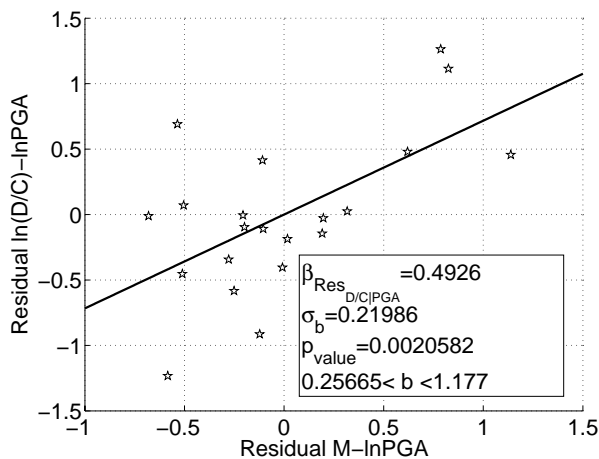


Figure 7. Residual-residual plot for magnitude as a second independent variable for predicting the structural response.

Judging from both the p-value and the reported b value, a significant positive trend in the plot can be observed: this means that peak ground acceleration is not sufficient with respect to the magnitude.

Figure 8 shows the results obtained by the cloud method and the introduction of magnitude, using the multiple regression.

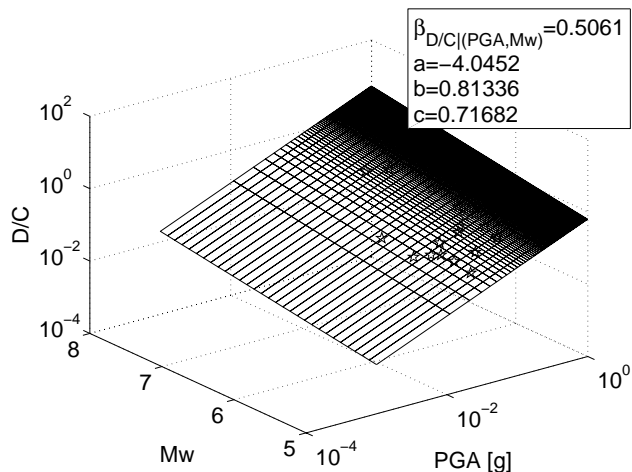


Figure 8. Multiple regression PGA-M-D/C (*Sel\_A*).

As mentioned previously, an alternative method based on weighting the results of the non linear dynamic analysis with the results of seismic hazard disaggregation is shown in Figure 9; results of structural analysis are plotted by circles with areas proportional to the corresponding weight.

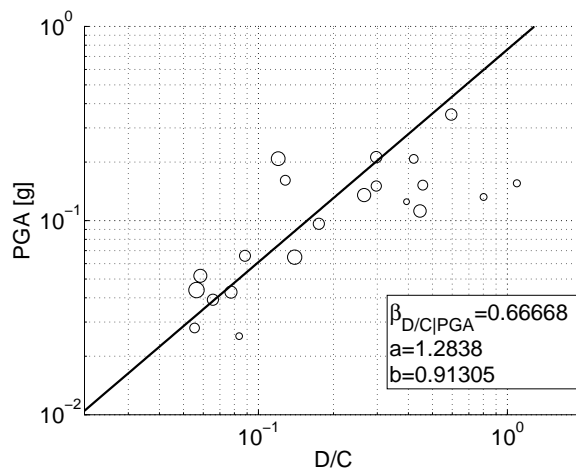


Figure 9. Weighted regression PGA-D/C-M (*Sel\_A*).

It would be interesting to study how the probability distribution for the displacement-based response is going to be affected by the weighed regression scheme. Moreover, in order to be able to judge if the weighted regression is helpful in adjusting for the dependence on magnitude, the hazard curve for the displacement-based response has been calculated with the pair [PGA, M] as the intensity measure. Figure 10 illustrates the hazard curve calculated following the above mentioned alternative methods.

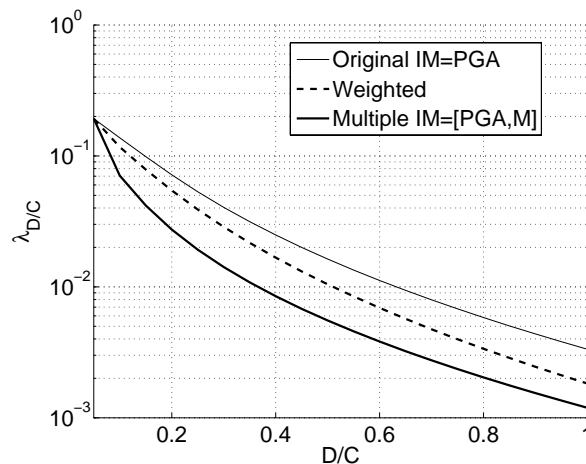


Figure 10. Hazard curves (cloud) (*Sel\_A*).

The thick line represents the hazard curve using the pair [PGA, M] as the intensity measure, the thin line represents the hazard curve using PGA as the intensity measure, and the dashed line represents the hazard curve using PGA as the intensity measure but adjusting for the dependence on magnitude by weighted regression. The position of the hazard curve calculated using the weighted regression indicates that the weighting scheme is effective for taking into account the magnitude dependence in the prediction of hazard for the displacement-based response.

### 10.1.2 Record selection B (Sel\_B)

For record selection B (*Sel\_B*) the primary intensity measure used in this study in scalar form is the first-mode spectral acceleration ( $S_a(T_1)$ ), then paired in vector form, with the deviation from the attenuation prediction epsilon ( $\epsilon$ ). In Figure 11 are shown the results obtained from structural dynamics using the cloud method for the  $S_a(T_1)$  and D/C.

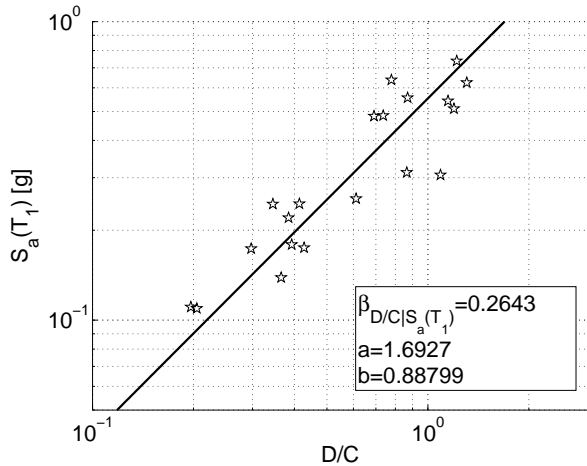


Figure 11. Simple regression  $S_a(T_1)$ -D/C (*Sel\_B*).

In order to establish sufficiency of the primary intensity measure and the effectiveness of ground motion characteristic variables as additional regression variables, the residual-residual plot is used. In Figure 12 is shown the residual-residual plot related to the introduction of epsilon as additional intensity measure, and the p-values obtained from hypotheses test.

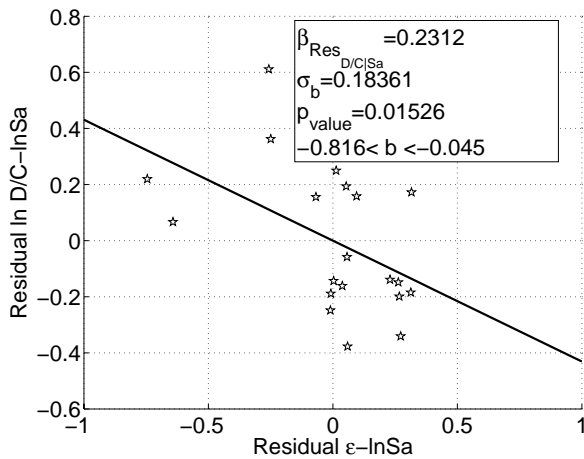


Figure 12. Residual-residual plot for epsilon as a second independent variable for predicting the structural response.

Judging from both the p-value and the reported sigma value, a negative trend can be observed: this means that first-mode spectral acceleration is not sufficient with respect to the epsilon. Figure 13 shows the results obtained by the cloud method and the introduction of epsilon, using the multiple regression.

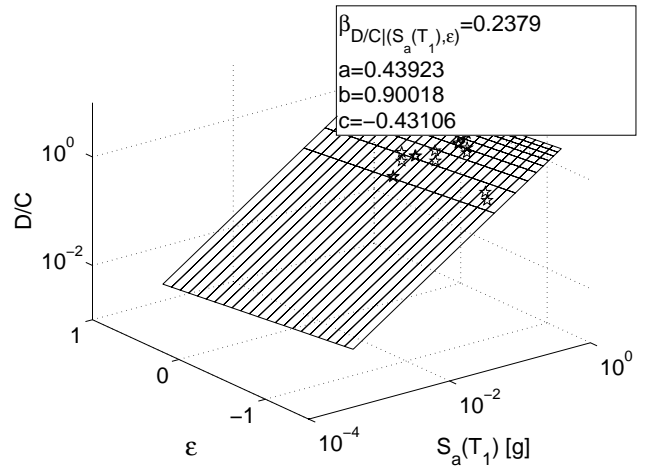


Figure 13. Multiple regression  $S_a(T_1)$ - $\epsilon$ -D/C (*Sel\_B*).

An alternative method based on weighting the results of the non linear dynamic analysis with the results of seismic hazard disaggregation is shown in Figure 14; results of structural analysis are plotted by circles with areas proportional to the corresponding weight.

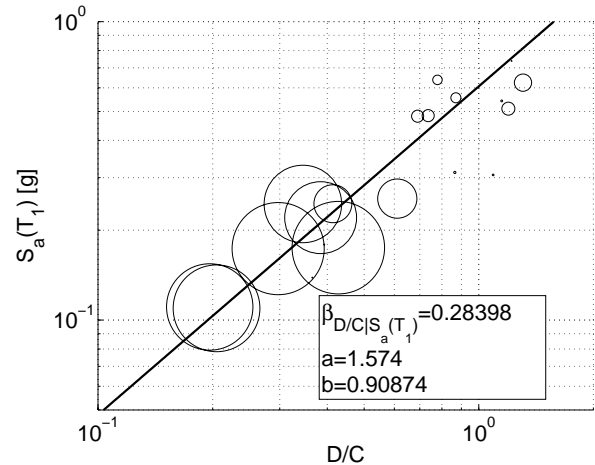


Figure 14. Weighted regression  $S_a(T_1)$ -D/C- $\epsilon$  (*Sel\_B*).

Figure 15 illustrates the hazard curve calculated with the different methods.

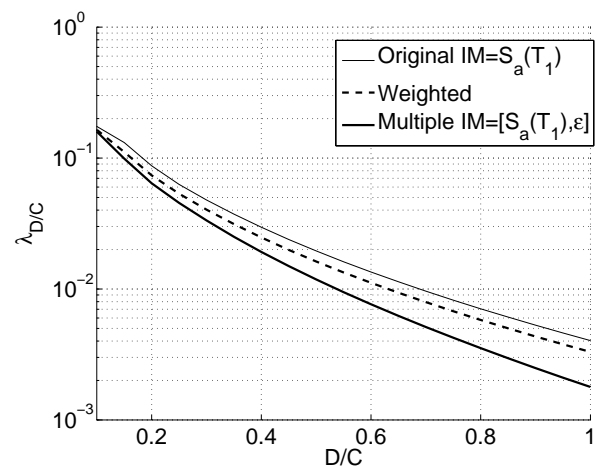


Figure 15. Hazard curves (cloud) (*Sel\_B*).

Also in this case the position of the hazard curve calculated using the weighted regression



indicates that the weighting scheme is effective for taking into account the epsilon dependence in the prediction of hazard for the displacement-based response.

### 10.2 Multiple-stripe Analysis

In this section, the results of multiple-stripe analysis are used in order to investigate the efficacy of the weighting scheme based on the disaggregation of the hazard, for the prediction of hazard for the displacement-based response using the same intensity measures used in the cloud method.

#### 10.2.1 Record selection A (*Sel\_A*)

Figure 16 illustrates the results of multiple-stripe analysis for the structure herein considered subjected to record selection A.

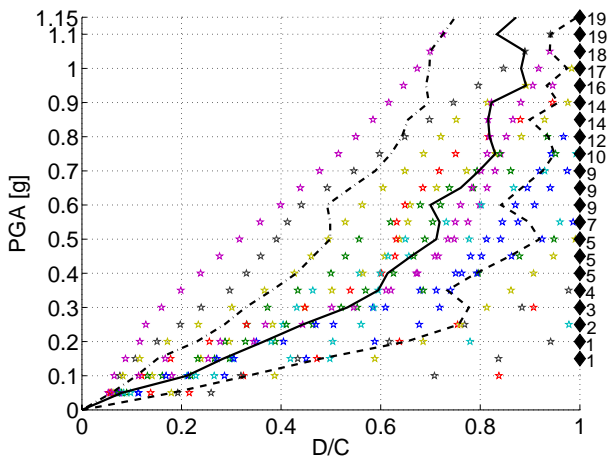


Figure 16. Multiple-stripe analysis (*Sel\_A*).

The lines connecting the (counted) 16th, 50th and 84th percentiles of the stripes are also shown in Figure 16; numbers near black diamonds indicate the number of collapse cases for each level of PGA. Figure 17 illustrates the hazard curve calculated employing the different methods.

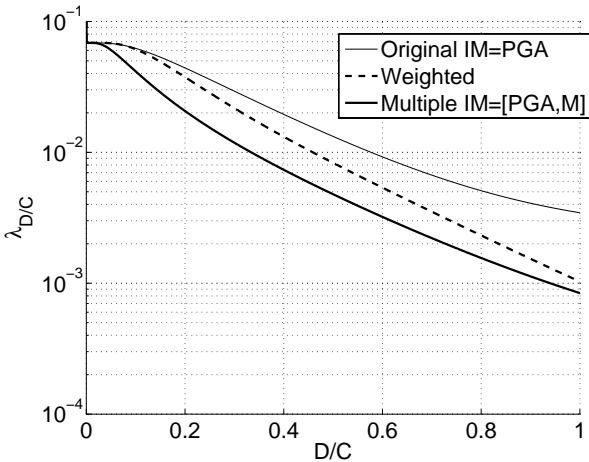


Figure 17. Hazard curves (stripes) (*Sel\_A*).

Also with the multiple-stripe method the position of the hazard curve calculated using the weighted method indicates that the weighting scheme is effective in taking into account the magnitude dependence in the prediction of hazard for the displacement-based response.

#### 10.2.2 Record selection B (*Sel\_B*)

Figure 18 illustrates the results of multiple-stripe analysis for the structure herein considered subjected to record selection B.

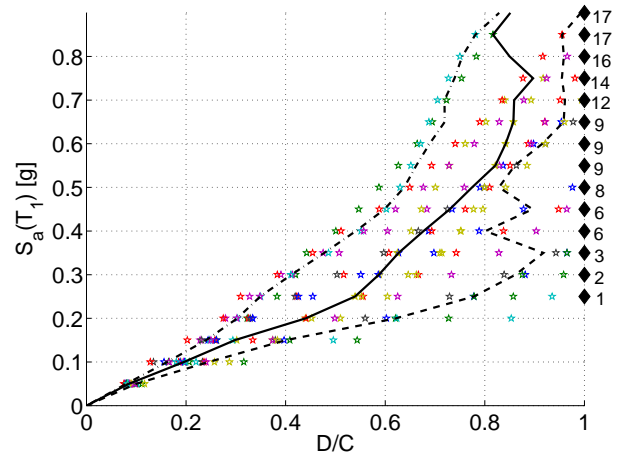


Figure 18. Multiple-stripe analysis (*Sel\_B*).

The lines connecting the (counted) 16th, 50th and 84th percentiles of the stripes are also shown in Figure 18; numbers near black diamonds indicate the number of collapse cases for each level of  $S_a(T_1)$ . Figure 19 illustrates the hazard curve calculated with the different methods.

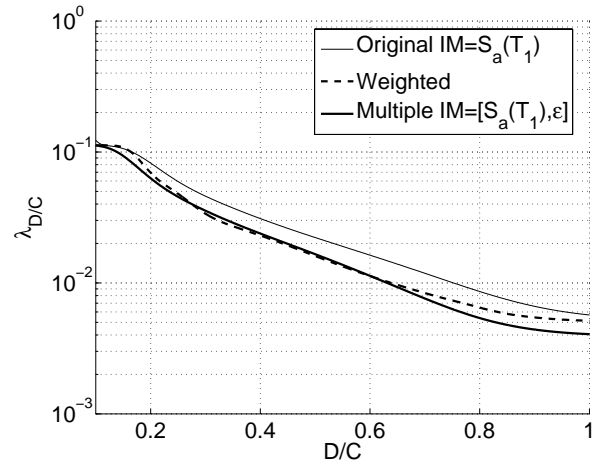


Figure 19. Hazard curves (stripes) (*Sel\_B*).

Similar to cloud method, the results of the multiple-stripe method indicate that hazard curve obtained using the weighted scheme is reasonably close to that based on multiple regression and vector  $[S_a(T_1), \epsilon]$ .

## 11 CONCLUSIONS

It is argued that, theoretically speaking, careful record selection is not essential if the candidate intensity measure (IM) is demonstrated to be “sufficient” with respect to the ground motion characteristic variables. “Sufficiency” (Luco and Cornell, 2001) is a probabilistic criterion for a preferred IM, in which the structural (displacement-based) response for a given IM level is conditionally statistically independent of the ground motion characteristics variables. Linear regression was used as the statistical tool for investigating the sufficiency of the candidate IM. In the cases where sufficiency for the candidate IM could not be established, a weighted regression scheme based on the results of the seismic hazard disaggregation for the ground motion characteristic variable(s) was implemented in order to adjust for the observed dependencies.

Two alternative non-linear dynamic analysis procedures have been considered in this work. The implication of using the weighted regression has been studied in terms of the annual frequency of exceedance of the critical component demand to capacity in an existing reinforced concrete structure using both the first-mode spectral acceleration and the peak ground acceleration as intensity measures.

Among all the analysed cases the estimated hazard curve for the displacement-based response using the weighted regression method has been close to the one derived by adopting a vector-valued intensity measure and using multiple regression. It is to be noted that the probabilities of collapse obtained with the cloud method and the two record selections are very similar when the weighted method or the multiple regression is used. The same observation can be made with the results of the multiple-stripe method; moreover, as expected in considering the increased sophistication of the method and the additional computational effort, the estimation of the probability of collapse obtained through multiple-stripe method, for the analysed structure improves.

In conclusion, it has been observed that the weighted regression enhances the hazard estimations for the displacement-based response for the structure considered herein.

## REFERENCES

Baker JW, Cornell CA. A vector-valued ground motion intensity measure consisting of spectral acceleration and

epsilon. *Earthquake Engineering & Structural Dynamics*, 34:1193-1217, 2005.

Baker JW. Probabilistic structural response assessment using vector-valued intensity measures. *Earthquake Engineering & Structural Dynamics*, 36 (13) 1861-1883, 2007.

Bazzurro, P., Cornell CA., (1998), Disaggregation of seismic hazard, *Bulletin of the Seismological Society of America*, 89, 2, Apr. 1999, pages 501-520.

Ditlevsen O, Masden H. *Structural Reliability Methods*, June 1996; John Wiley & Sons Inc.

Iervolino I, Cornell C.A. (2005). Record selection for nonlinear seismic analysis of structures. *Earthquake Spectra*, 21(3):685-713.

Jalayer F. Direct Probabilistic Seismic Analysis: Implementing Non-linear Dynamic Assessments, *Ph.D. Thesis, Department of Civil and Environmental Engineering, Stanford, CA*, March 2003.

Jalayer, F., and Cornell, C. A. (2008), Alternative Nonlinear Demand Estimation Methods for Probability-Based Seismic Assessments, *Earthquake Engineering and Structural Dynamics*, 2008.

Luco, N. and Cornell, C.A.(2001). Structure-specific scalar intensity measures for near-source and ordinary earthquake ground motions, *Earthquake Spectra*.

McGuire RK. Seismic Hazard and Risk Analysis. *Earthquake Engineering Research Institute*; First Edition, August 2004.

Neter, J., Kutner, M. H., Nachtsheim, C. J., and Wasserman, W., (1996). *Applied linear statistical models*, (McGraw-Hill, Boston).

Ordinanza del Presidente del Consiglio dei Ministri (OPCM), Norme tecniche per il progetto, la valutazione e l'adeguamento sismico degli edifici esistenti. n. 3431, maggio 2005 (in Italian).

Regio Decreto Legge (R.D.L.) 2229. Norme per l'esecuzione delle opere in conglomerato cementizio semplice o armato, 1939 (in Italian).

Sabetta F, Pugliese A. Estimation of response spectra and simulation of non-stationary earthquake ground motions. *Bulletin of the Seismological Society of America*, 86(2):337-352, April 1996.

Scott MH, GL Fennes. Plastic hinge integration methods for force-based beam-column elements, *Journal of Structural Engineering, ASCE*, 132(2):244-252, February 2006.

Shome, N., and Cornell, C.A. (1999). Probabilistic seismic demand analysis of non-linear structures. *Report No. RMS-35, Stanford University, Stanford, CA*.

Weisberg, S., (1985), *Applied linear regression*, John Wiley & Sons., Second Edition.